

Lyapunov instability of two-dimensional fluids: Hard dumbbells

Lj. Milanović and H. A. Posch

Institut für Experimentalphysik, Universität Wien, Boltzmannngasse 5, A-1090 Wien, Austria

Wm. G. Hoover

Department of Applied Science, University of California at Davis/Livermore and Lawrence Livermore National Laboratory, Livermore, California 94551-7808

(Received 20 November 1997; accepted for publication 27 February 1998)

We generalize Benettin's classical algorithm for the computation of the full Lyapunov spectrum to the case of a two-dimensional fluid composed of linear molecules modeled as hard dumbbells. Each dumbbell, two hard disks of diameter σ with centers separated by a fixed distance d , may translate and rotate in the plane. We study the mixing between these qualitatively different degrees of freedom and its influence on the full set of Lyapunov exponents. The phase flow consists of smooth streaming interrupted by hard elastic collisions. We apply the exact collision rules for the differential offset vectors in tangent space to the computation of the Lyapunov exponents, and of time-averaged offset-vector projections into various subspaces of the phase space. For the case of a homogeneous mass distribution within a dumbbell we find that for small enough d/σ , depending on the density, the translational part of the Lyapunov spectrum is decoupled from the rotational part and converges to the spectrum of hard disks. © 1998 American Institute of Physics.

[S1054-1500(98)01002-7]

The Lyapunov spectrum characterizes many-body Lyapunov instability just as the single Lyapunov exponent describes a single chaotic degree of freedom. Computer simulations of atomistic fluids and solids, as well as continuum flows, have revealed a rich variety of spectra, well beyond the reach of current theory. Here we extend the atomistic simulations to the simplest model for a diatomic fluid in two dimensions, identical hard dumbbells interacting according to classical mechanics. The anisotropy-dependent spectrum for the dumbbell fluid reflects the physical transition from uncoupled translational and rotational motions to fully coupled rotational states. We also demonstrate that the eigenvectors, which characterize the many-body Lyapunov spectra, can correspond to localized excitations.

I. INTRODUCTION

During the last decade, the spectrum of Lyapunov exponents for many-body systems has been the focus of extensive numerical simulations and of interesting theoretical studies. The motivations for this interest are numerous. Lyapunov exponents are the time-averaged rate constants for the exponential divergence and convergence of neighboring phase-space trajectories and, thus, an indicator for dynamical chaos.¹ For more than a few degrees of freedom they provide the only practical method for determining the dimension of fractal attracting structures in the phase space measure of nonequilibrium steady-state systems.^{2,3} They have been instrumental for our understanding of the second law of thermodynamics and the macroscopic irreversible behavior of such systems.^{4,5} Furthermore, they are related to the transport coefficients and offer new bases for discussing transport.^{6,7} Also equilibrium Lyapunov spectra have provided new and

unexpected insights. It was recognized that the shape of the spectrum varies considerably with the state of the system^{2,8} and that the maximum exponent becomes maximal, as a function of the density, or changes discontinuously, as a function of the energy, at a phase transition. Examples include the fluid–solid transition in two or three physical dimensions,^{9–12} and the orientational disorder–order transition for an extended XY model of planar rotators.^{13,14} Theoretical arguments have been given by Sinai for the existence of the Lyapunov spectrum in the thermodynamic limit of infinitely many particles, interacting with a pairwise additive short-range potential.¹⁵ They are based on the assumption that the thermodynamic-limit transition $N \rightarrow \infty$ is taken before the time-average limit $t \rightarrow \infty$. Most numerical and theoretical results are in support of this expectation.^{16–18} However, a weak, but very persistent, increase of the maximum exponent with the particle number N has been interpreted recently as a possible logarithmic singularity.¹⁹ Thus, the study of the Lyapunov instability adds complementary information to more established views of the dynamical properties of many-body systems.

We have recently generalized the classical algorithms by Benettin *et al.*²⁰ and Shimada *et al.*²¹ to study hard disk¹⁷ and hard sphere¹⁸ systems in two and three dimensions, respectively. These systems are paradigms for fluids and can be treated by kinetic theory. Within this framework van Beijeren *et al.*²² formulated the first successful analytical theory for the Kolmogorov–Sinai entropy, expressed as the sum of all positive Lyapunov exponents, for low-density gases. In another, although related, approach van Zon *et al.*²³ succeeded in computing the maximum Lyapunov exponent. In numerical work, the advantages of low-density studies, with a very good signal-to-noise ratio, typical for hard elastic interactions, are recovered.

So far, almost all computations of Lyapunov spectra for many-body systems involve *atomic* systems. The only exception we are aware of is due to Borzsák, Posch, and Baranyai,²⁴ who studied *molecular* fluids composed of rigid diatomic molecules with two interaction sites per molecule, interacting with a soft repulsive site-site potential. This simulation provided the first study of a system affected by both translational and rotational degrees of freedom. Here we introduce an extension of our hard-disk algorithm and study a two-dimensional system of N hard dumbbells. Each dumbbell consists of two rigidly connected hard disks of diameter σ and center-center separation $d \leq \sigma$. Numerically the advantages of a very good signal-to-noise ratio, typical for hard elastic interactions, are recovered. It also permits the study of low-density gases. There are various possibilities for the mass distribution within a dumbbell, which lead to different moments of inertia for a given molecular anisotropy d/σ . The simplest model assumes that the mass of a disk is concentrated in its center (point-mass dumbbells). It is the limiting case of the soft diatomic-molecule model mentioned above. Work on the point-mass dumbbells and a comparison with the respective soft case will appear elsewhere.²⁵ In this paper we assume that the total dumbbell mass is homogeneously distributed over the whole dumbbell, i.e., the union of the two connected disks (homogeneous dumbbells).

The paper is organized as follows. In Sec. II we introduce our model and summarize its collision dynamics in phase space. In Sec. III we describe our exact method for the computation of the full Lyapunov spectrum in tangent space. We define certain projections of the tangent-space dynamics into subspaces spanned only by variables associated with (i) translational, and (ii) rotational degrees of freedom, or (iii) with the phase space of single particles. These projections allow a very detailed analysis of our results, which is presented in Sec. IV. We discuss the extent to which the translational and rotational degrees are involved in the dynamics of the tangent vectors belonging to the various Lyapunov exponents. To save space we restrict our attention to a low-density gas and discuss in detail the onset of coupling between rotation and translation. In the concluding Sec. V we demonstrate that the molecules most active in the stretching and contraction dynamics in tangent space at any instant of time are very localized in physical space and form "macroscopic modes," which are not directly correlated with other particle properties such as temperature, energy and stress.

II. SIMULATION OF HOMOGENEOUS DUMBBELLS

We consider a planar and purely classical system of N hard dumbbells in a square simulation box with periodic boundary conditions. Each dumbbell, sometimes also referred to as a "molecule," consists of two rigidly connected disks separated by d . Each disk has a diameter σ and a mass $m/2$. The molecular mass m is assumed to be homogeneously distributed over the union of the two disks. The moment of inertia for rotation around the center of mass becomes

$$I = \begin{cases} \frac{m\sigma^2}{4} \frac{3dw + [d^2 + (\sigma^2/2)][\pi + 2 \arctan(d/w)]}{2dw + \sigma^2[\pi + 2 \arctan(d/w)]} & \text{if } d \leq \sigma \\ \frac{m}{4} \left[\frac{\sigma^2}{2} + d^2 \right] & \text{if } d > \sigma, \end{cases} \quad (1)$$

where $w = \sqrt{\sigma^2 - d^2}$ is the molecular waist. For $d \rightarrow 0$ this moment of inertia converges to that of a single disk with mass m and diameter σ , and with a homogeneous mass density.

The state of a dumbbell i is given by $\mathbf{r}_i, \mathbf{p}_i, \alpha_i$, and J_i , where \mathbf{r}_i and \mathbf{p}_i refer to the position and linear momentum of its center of mass, respectively, α_i denotes the orientation angle between the separation vector of the two disk centers with an arbitrary fixed direction of the plane, and J_i is the angular momentum with respect to rotation around the center of mass. Between collisions the state changes according to

$$\dot{\mathbf{r}}_i = \mathbf{p}_i/m; \quad \dot{\mathbf{p}}_i = \mathbf{0}; \quad \dot{\alpha}_i = J_i/I; \quad \dot{J}_i = 0. \quad (2)$$

It is convenient for the following to introduce the $6N$ -dimensional state vector in phase space, $\Gamma = \{\mathbf{r}_i, \mathbf{p}_i, \alpha_i, J_i\}; i = 1, \dots, N$, and to write the motion equations (2) for intercollisional streaming according to

$$\dot{\Gamma} = \mathbf{F}(\Gamma).$$

To find successive collisions we integrate these equations with a time step Δt and check for overlap of two molecules. In such an event the collision point is determined iteratively with an accuracy $< 10^{-12}\sigma$. For all details we refer to Ref. 26. At each collision the collision map

$$\begin{aligned} \mathbf{r}_i^+ &= \mathbf{r}_i^-, & \mathbf{r}_j^+ &= \mathbf{r}_j^-, \\ \mathbf{p}_i^+ &= \mathbf{p}_i^- + \Delta \mathbf{p}, & \mathbf{p}_j^+ &= \mathbf{p}_j^- - \Delta \mathbf{p}, \\ \alpha_i^+ &= \alpha_i^-, & \alpha_j^+ &= \alpha_j^-, \\ J_i^+ &= J_i^- + [\mathbf{r}_{ci} \times \Delta \mathbf{p}]_0, & J_j^+ &= J_j^- - [\mathbf{r}_{cj} \times \Delta \mathbf{p}]_0 \end{aligned} \quad (3)$$

is applied to the colliding molecules, where the superscripts $-$ and $+$ refer to states immediately before and after the collision, respectively. \mathbf{r}_{ci} is the relative position vector of the collision point with respect to the center of mass of molecule i . The notation $[\mathbf{a}]_0$ denotes the component of a three-dimensional vector \mathbf{a} perpendicular to the simulation plane. The map (3) is a consequence of the conservation laws for energy, linear momentum and angular momentum, and the condition that the colliding surfaces are smooth. This smoothness condition requires that the momentum change $\Delta \mathbf{p} = \Delta p \mathbf{n}$, where \mathbf{n} is a unit vector pointing from the center of the colliding disk for molecule i to that of molecule j . Furthermore,

$$\Delta p = \frac{(\mathbf{p}_j - \mathbf{p}_i) \cdot \mathbf{n} / m + \{[\mathbf{r}_{cj} \times \mathbf{n}]_0 J_j^- - [\mathbf{r}_{ci} \times \mathbf{n}]_0 J_i^-\} / I}{1/m + \{[\mathbf{r}_{ci} \times \mathbf{n}]^2 + [\mathbf{r}_{cj} \times \mathbf{n}]^2\} / 2I}.$$

The collision map (3), augmented by the unaffected state variables of the other molecules not partaking in this collision, is conveniently abbreviated according to

$$\Gamma^+ = \mathbf{M}(\Gamma^-). \quad (4)$$

III. LYAPUNOV EXPONENTS

The phase trajectory of a chaotic system is extremely sensitive to small perturbations of the initial conditions, which means that two phase points, initially separated by a small distance in phase space, diverge or converge exponentially. The time-averaged exponential rates of divergence (convergence) are referred to as the Lyapunov exponents,

$$\lambda(\delta\Gamma(0)) = \lim_{t \rightarrow \infty} \frac{1}{t} \ln \frac{|\delta\Gamma(t)|}{|\delta\Gamma(0)|}, \quad (5)$$

where the tangent vector $\delta\Gamma(t)$ gives the infinitesimal displacement of a perturbed satellite trajectory from the reference trajectory $\Gamma(t)$. According to Oseledec²⁷ there are L orthonormal initial vectors $\delta\Gamma_k(0)$ yielding a set of exponents, the Lyapunov spectrum $\{\lambda_k\}, k=1, \dots, L$, which is taken to be ordered such that $\lambda_k \geq \lambda_{k+1}$. L is equal to $6N$, the phase space dimension.

To compute the Lyapunov exponents for hard dumbbell systems we follow Dellago *et al.*,^{17,18} who generalized Benettin's classical algorithm^{20,21,28} to hard disk and hard sphere systems. The method requires the construction of as many offset vectors in tangent space as Lyapunov exponents are required. For the streaming between collisions each $\delta\Gamma(t)$ is a solution of the linearized equations

$$\dot{\delta\Gamma} = (\partial\mathbf{F}/\partial\Gamma) = \{\delta\mathbf{p}_i/m, \mathbf{0}, \delta J_i/I, 0\}^T; i=1, \dots, N,$$

where T means transposition. The linearization, in time and phase space coordinates, for the collision map (4) yields¹⁷

$$\delta\Gamma^+ = \frac{\partial\mathbf{M}}{\partial\Gamma} \cdot \delta\Gamma^- + \left[\frac{\partial\mathbf{M}}{\partial\Gamma} \cdot \mathbf{F}(\Gamma^-) - \mathbf{F}(\mathbf{M}(\Gamma^-)) \right] \delta\tau_c. \quad (6)$$

With these expressions it is possible to compute the exact time evolution of any tangent vector $\delta\Gamma(t)$ and to obtain the full Lyapunov spectrum from Eq. (5).

The matrix $\partial\mathbf{M}/\partial\Gamma$ in Eq. (6) is symbolically evaluated with the analytical package MUPAD,²⁹ and the computer code for the matrix elements, generated by MUPAD in the C programming language, is used directly in our program. $\delta\tau_c$ is the (positive or negative) time delay between the collision of the satellite trajectory with respect to that of the reference trajectory. The distance between the centers of the colliding disks is given by $\mathbf{r}_d = \mathbf{r}_j + \mathbf{k}_j - \mathbf{r}_i - \mathbf{k}_i$, and its variation for the satellite trajectory with respect to the reference trajectory by $\delta\mathbf{r}_d = \delta\mathbf{r}_j + \delta\mathbf{k}_j - \delta\mathbf{r}_i - \delta\mathbf{k}_i$. Here, \mathbf{k}_i is the vector from the center of mass of molecule i to its disk involved in the collision, for which

$$\mathbf{k}_i = \frac{d}{2} \begin{pmatrix} \cos \alpha_i \\ \sin \alpha_i \end{pmatrix},$$

$$\delta\mathbf{k}_i = \frac{d}{2} \begin{pmatrix} -\delta\alpha_i \sin \alpha_i \\ \delta\alpha_i \cos \alpha_i \end{pmatrix} = \delta\alpha_i \begin{pmatrix} 0 & -1 \\ 1 & 0 \end{pmatrix} \mathbf{k}_i.$$

Then, the time delay $\delta\tau_c$ is given by

$$\delta\tau_c = - \frac{\delta\mathbf{r}_d \cdot \mathbf{n}}{\mathbf{v}_d \cdot \mathbf{n}}, \quad (7)$$

the component of $\delta\mathbf{r}_d$ perpendicular to the collision surface, divided by the relative normal velocity of the colliding disks. For the relative disk velocity we have $\mathbf{v}_d \equiv \mathbf{v}_{j,d} - \mathbf{v}_{i,d}$, where

$$\mathbf{v}_{i,d} = \mathbf{v}_i + \omega_i \begin{pmatrix} 0 & -1 \\ 1 & 0 \end{pmatrix} \mathbf{k}_i$$

is the velocity of the colliding disk for molecule i in the laboratory frame.

The tangent vectors are reorthonormalized after every five collisions, and the Lyapunov exponents are computed from the time-averaged logarithms of the renormalizing factors.^{20,28} Since the phase volume is conserved, any expansion in certain phase-space directions is exactly compensated by a contraction in some other directions, and the sum of all Lyapunov exponents must vanish. As a consequence of the time-reversal invariance of the equations of motion, the Lyapunov exponents appear in conjugate pairs of equal magnitude and opposite sign. In all our examples we have computed the full spectrum of exponents and have verified the pairing rule with high precision. In the figures only the positive branches of the spectra are shown. The conservation of energy, of linear momentum, of the center of mass, and the neutral expansion behavior in the flow direction cause three conjugate exponent pairs to vanish. The various pairs are specified by an index l such that the most positive and negative exponents, λ_1 and λ_{6N} , are associated with $l=1$, the second-largest exponent λ_2 and second-smallest exponent λ_{6N-1} with $l=2$, and, finally, the six vanishing exponents $\lambda_{3N-2}, \dots, \lambda_{3N+3}$ with the indices $3N-2$ to $3N$.

A more detailed analysis of the dynamics in tangent space is possible if projections of the tangent vectors $\delta\Gamma_l$ into various orthogonal subspaces, $TX \in \{T\mathbf{r}, T\mathbf{p}, T\alpha, TJ\}$, are considered. The projections are associated with the center-of-mass configuration space \mathbf{r} , the translational momentum space \mathbf{p} , the space of the molecular orientation angles α , and the space of angular momenta J , respectively.²⁴ If $\delta\Gamma_{X,l}$ denotes a tangent space vector with components identical to those of $\delta\Gamma_l$ for directions belonging to TX , and vanishing otherwise, the time-averaged squared length

$$\delta_{X,l}^2 \equiv \langle \delta\Gamma_{X,l} \cdot \delta\Gamma_{X,l} \rangle \quad (8)$$

is taken as a measure for the probability of $\delta\Gamma_l$ of pointing into a direction of tangent space belonging to the selected subspace TX . These so-called "mean-squared X components"²⁴ are directly related to the coherence angles introduced by D'Alessandro and Tenenbaum.³⁰

Another application of the same idea is to project into the single-particle subspaces $T\mu_i$ spanned by $\delta\mathbf{r}_i, \delta\mathbf{p}_i, \delta\alpha_i, \delta J_i$, for $i=1, \dots, N$,⁵

$$\delta_{\mu_i,l}^2(t) \equiv (\delta\mathbf{r}_i)_l^2 + (\delta\mathbf{p}_i)_l^2 + (\delta\alpha_i)_l^2 + (\delta J_i)_l^2. \quad (9)$$

No time averaging is applied in this case. This allows us to determine what molecules participate most in the stretching or collapsing processes at some instant of time, and whether or not these processes are homogeneously distributed or localized in physical space.

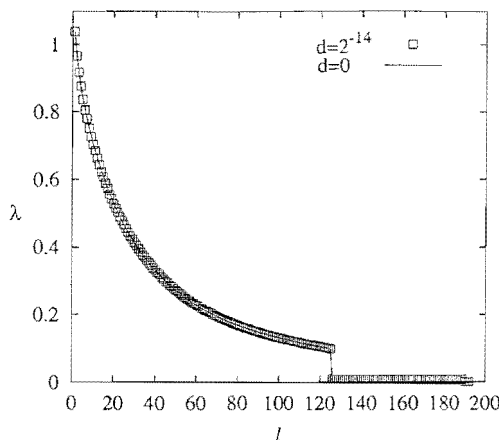


FIG. 1. The squares denote the positive branch of the Lyapunov spectrum of a planar system consisting of $N=64$ homogeneous dumbbells with a molecular anisotropy $d/\sigma=2^{-14}$. The density $n=0.1\sigma^{-2}$. The smooth curve refers to an equivalent spectrum of 64 hard disks ($d=0$) without rotational degrees of freedom. The index on the abscissa labels conjugate exponent pairs, which are defined only for integer indices. For $d=0$ there are only $2N=128$ exponent pairs and six vanishing exponents, associated with the indices 126 to 128. The Lyapunov exponents are given in units of $\sqrt{(K/N)/(m\sigma^2)}$, where K is the total (kinetic) energy, m is the dumbbell mass, and σ is the diameter of the two rigidly connected disks forming a dumbbell.

IV. RESULTS

In all our numerical work we use reduced units for which the disk diameter σ , the molecular mass m , the specific energy $E/N(=K/N)$ and the Boltzmann constant k are equal to unity. The unit of time is $\sqrt{m\sigma^2 N/K}$, where K is the total kinetic energy. The number density of the system is defined by $n=N/V$ where V is the area of the simulation box.

Here we consider systems consisting of 64 dumbbells with a molecular anisotropy d/σ . All systems are low-density gases, $n=0.1\sigma^{-2}$, for which we study the onset of coupling between translational and rotational degrees of freedom. The low density was chosen to avoid complications from fluid to solid phase transitions. Work on denser systems is in progress.²⁵

For homogeneous dumbbells the moment of inertia, for $d \rightarrow 0$, remains finite, and the Lyapunov spectra are well behaved. In Fig. 1 the positive branch of the spectrum, or more precisely half of the exponents, for a 64-dumbbell system with an anisotropy ratio $d/\sigma=2^{-14}$ is shown by the squares. The smooth line represents analogous data for a system of 64 disks ($d=0$), which has only translational and no rotational degrees of freedom and which are taken from our previous work.¹⁷ To facilitate this comparison we note that in Ref. 17 the unit of energy was defined by the translational kinetic energy per particle, whereas here it is the sum of the translational and rotational kinetic energies per particle. Thus, the unit of time in Ref. 17 differs by a factor of $\sqrt{(2N-2)/(3N-2)}$ from the unit used here, which must be taken into account in comparing Lyapunov exponents. From the impressive agreement between these two sets of data in Fig. 1 we conclude that for a small enough, but finite, anisotropy d the Lyapunov exponents associated with the transla-

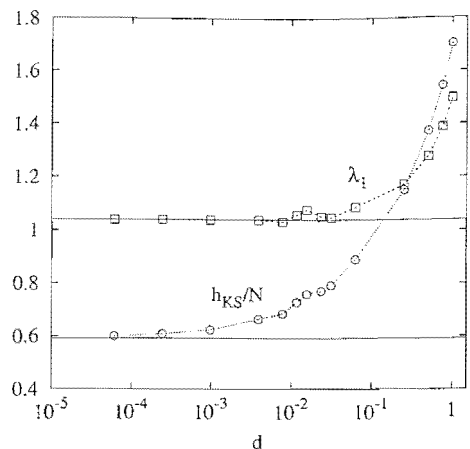


FIG. 2. Maximum Lyapunov exponent λ_1 and Kolmogorov-Sinai entropy per particle, h_{KS}/N , for a 64-dumbbell system of density $n=0.1\sigma^{-2}$, as a function of the anisotropy d/σ . d is given in units of σ , and λ_1 and h_{KS} in units of $\sqrt{(K/N)/(m\sigma^2)}$. The horizontal smooth lines are results for hard disks taken from Ref. 17.

tional degrees of freedom are decoupled from those for molecular reorientation. The total spectrum decomposes into a translational part $1 \leq l \leq 125$, and a rotational part $126 \leq l \leq 189$. The vanishing exponents belong to the indices $190 \leq l \leq 192$.

In Fig. 2 the dependence of the maximum exponent, λ_1 , and of the Kolmogorov-Sinai entropy per particle h_{KS}/N , on the molecular anisotropy d/σ are shown. These quantities converge very well, for $d \rightarrow 0$, to their purely translational hard disk limit, taken from Ref. 17 and indicated by the horizontal lines, but are considerably enhanced by rotation for larger d . It is significant that the convergence is complete for λ_1 already for values of d for which h_{KS} , the sum of all positive exponents, is not converged yet. This is due to the ‘rotational part’ of the spectrum in Fig. 1 also contributing to h_{KS} . For $d \leq 10^{-3}\sigma$ the positive branch of the rotational part consists of 64 exponents which are very close to each other. This may be inferred from Fig. 3, where we have

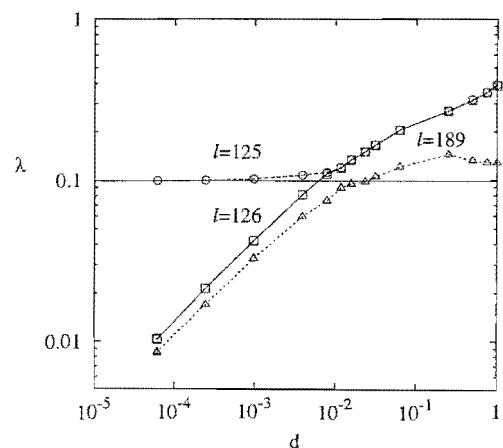


FIG. 3. Anisotropy dependence of selected positive Lyapunov exponents, labeled by their index l , for a 64-dumbbell system of density $n=0.1\sigma^{-2}$. d is given in units of the disk diameter σ , and the λ_l in units of $\sqrt{(K/N)/(m\sigma^2)}$. The horizontal line indicates the value of the smallest positive exponent for the spectrum of 64 hard disks taken from Ref. 17.

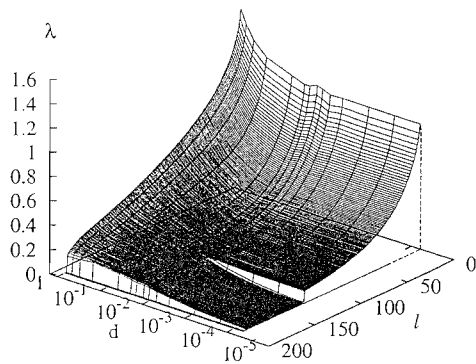


FIG. 4. Anisotropy dependence for the positive branch of the Lyapunov spectrum for a 64-dumbbell system at a density $n=0.1\sigma^{-2}$. d is given in units of the disk diameter σ , and λ in units of $\sqrt{(K/N)/(m\sigma^2)}$. The exponents are only defined for integer indices l .

plotted the smallest positive ($l=189$) and largest ($l=126$) of the “rotational” exponents as a function of d . We note that they scale $\sim d^{1/2}$ for $d \rightarrow 0$ as is indicated by the limiting slope. Also shown in this figure is the d dependence for the exponent $l=125$, the smallest of the positive “translational” exponents. For $d < 10^{-3}\sigma$ it is well converged to the smallest positive exponent for the purely translational disk system indicated by the horizontal line, whereas for $d > 10^{-2}\sigma$ it is very close to its neighbor, $l=126$, associated only with rotation for small d . We conclude that for $d < 10^{-3}\sigma$ the tangent space dynamics for translational motion is decoupled from that for reorientation. For $10^{-3}\sigma < d < 10^{-2}\sigma$ the coupling between translational and rotational degrees of freedom becomes more and more significant, and is essentially complete for a critical value $d_c \approx 10^{-2}\sigma$.

There is an interesting anomaly in these curves, which we believe is real and no artefact of the simulation. It is most clearly noticeable for the maximum exponent in Fig. 1. The maximum displayed there by λ_1 for molecular anisotropies close to the critical value d_c is indicative of unusually strong mixing in phase space. A similar behavior has been found for other order–disorder transitions.^{17,18,14,10} Apparently the

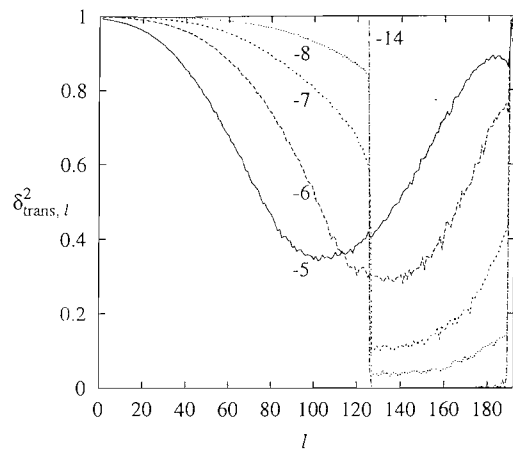


FIG. 5. Spectrum of the mean squared translational components for selected values of the anisotropy $d/\sigma=2^{-n}$, where $-n$ appears as a label on each curve. As usual, l is the Lyapunov index. The components are defined only for integer values of l .

transition to a coupled roto-translational state is analogous to a phase transition. We are currently investigating this point.

An overview of the shape dependence of the Lyapunov spectrum on d for constant number $n=0.1\sigma^{-2}$ is provided in Fig. 4. The decoupling between translational and rotational degrees of freedom is made clearly visible by the widening gap between the exponents $l=125$ and 126 for $d < 10^{-2}\sigma$. The increase of the exponents for large d is due to the smaller free volume and, hence, increased collision frequency. For later reference we tabulate in Table I the time-averaged translational and rotational kinetic energies, a few selected Lyapunov exponents, the Kolmogorov–Sinai entropy, and the single-particle collision rate, $1/\tau$, for the spectra appearing in Fig. 4.

The translational subspace of the tangent space is spanned by all $\delta\mathbf{r}_i, \delta\mathbf{p}_i$. The mean-squared components $\delta^2_{\text{trans},l}$ for projections into this subspace are shown in Fig. 5 for selected values of d indicated by the labels. We shall refer to them, for short, as “squared translational compo-

TABLE I. Simulation results for the Lyapunov spectra displayed in Fig. 4 for a 64-dumbbell system at a density of $n=0.1\sigma^{-2}$. d is the distance between the two disks of a dumbbell and is given in units of the disk diameter σ . The translational and rotational kinetic energies, K_T and K_R , are measured in units of the total kinetic energy per particle, $K/N=(K_T+K_R)/N$. h_{KS} is the Kolmogorov–Sinai entropy and is determined from the sum of all positive exponents. $1/\tau$ is the single-particle collision frequency. h_{KS} , $1/\tau$, and the selected Lyapunov exponents λ_l are all given in units of $[(K/N)/(m\sigma^2)]^{1/2}$, where m is the dumbbell mass.

d	K_T/N	K_R/N	h_{KS}/N	λ_1	λ_{125}	λ_{126}	λ_{189}	$1/\tau$
2^{-14}	0.667	0.333	0.599	1.038	0.099	0.010	0.0083	0.328
2^{-10}	0.660	0.340	0.623	1.038	0.101	0.042	0.0323	0.326
2^{-8}	0.660	0.340	0.663	1.037	0.107	0.081	0.0592	0.328
2^{-7}	0.642	0.358	0.684	1.031	0.112	0.109	0.074	0.324
$2^{-7}+2^{-8}$	0.678	0.322	0.727	1.057	0.120	0.119	0.089	0.333
2^{-6}	0.693	0.307	0.758	1.076	0.134	0.133	0.095	0.338
$2^{-6}+2^{-7}$	0.651	0.349	0.770	1.050	0.150	0.150	0.097	0.330
2^{-5}	0.652	0.348	0.791	1.047	0.165	0.165	0.105	0.330
2^{-4}	0.663	0.337	0.889	1.086	0.205	0.205	0.120	0.344
0.25	0.659	0.341	1.150	1.170	0.270	0.268	0.144	0.401
0.50	0.662	0.338	1.372	1.276	0.318	0.314	0.133	0.508
0.75	0.662	0.338	1.543	1.387	0.353	0.351	0.129	0.636
1.0	0.665	0.335	1.702	1.496	0.393	0.388	0.128	0.784

nents.” The analogous “squared rotational components,” obtained by projecting into the rotational subspace spanned by all $\delta\alpha_i, \delta J_i$, will be denoted by $\delta_{\text{rot},l}^2$. Obviously, $\delta_{\text{trans},l}^2 + \delta_{\text{rot},l}^2 = 1$, and each curve in Fig. 5 acts as a dividing line between a translational part below, and a complementary rotational part above. For $d = 2^{-14}\sigma$, labeled -14 in Fig. 5, all squared translational components are unity for $1 \leq l \leq 125$, and vanish for $126 \leq l \leq 189$. For the complementary squared rotational components it is reversed. The transition from $l = 125$ to 126 is *discontinuous*. For larger d the tangent vectors do not remain exclusively in one of these two subspaces, but start to spend more and more time also in the complementary subspace. The tangent vectors for the maximum and minimum exponents ($l=1$) are least affected. However, the discontinuous step between $l=125$ and 126 does not disappear until $d/\sigma \approx 2^{-6} \approx 0.016$, which is close to the critical value d_c found above. Only for $d > d_c$ one may speak of strong coupling between translational and rotational degrees of freedom.

We remark that the squared translational components for a conjugate pair of exponents are equal and that it is sufficient in Fig. 5 to consider the range of indices labeling exponent pairs. Such a symmetry, however, does not persist if, for example, projections into the position and momentum subspaces are considered separately. In such a case also the positive and negative branches of the Lyapunov spectra must be treated separately. An analogous remark also applies to the squared rotational components.

V. OUTLOOK

The existence of a discontinuous step in the spectrum of the squared translational and rotational coefficients for small molecular anisotropies is an unexpected result. The data presented here are for a number density $n = 0.1\sigma^{-2}$. We are working at present to extend these simulations to larger n and N to learn how the critical anisotropy ratio d_c/σ depends on the density and to characterize the effect of the fluid–solid phase transition on the spectrum. Another question concerns the existence of the thermodynamic limit, $N \rightarrow \infty$ for fixed n and K/N , for the spectra. It was shown for systems of hard disks in two dimensions,¹⁷ and for hard spheres in three,¹⁸ that the maximum exponent λ_1 seems to converge to a finite limit, although a logarithmic divergence cannot be completely ruled out, and that the ratio of the smallest positive exponent to the maximum exponent converges to zero. The existence of the thermodynamic limit for the Lyapunov spectrum has been conjectured for the one-dimensional Fermi–Pasta–Ulam chain (β model),¹⁶ and is expected, from purely theoretical arguments,^{15,23} also for higher-dimensional systems with pairwise short-range potentials. We have found finite limiting exponents also for two-dimensional systems in nonequilibrium steady states with up to 32000³¹ and 102400 particles.³² On the other hand, Searles *et al.*¹⁹ interpret a weak, but persistent, increase of λ_1 with N as a possible sign of a logarithmic divergence. Their simulations involved up to 8000 Weeks–Chandler–Anderson particles. In the present work the range of N values studied is not large enough to decide on this question.

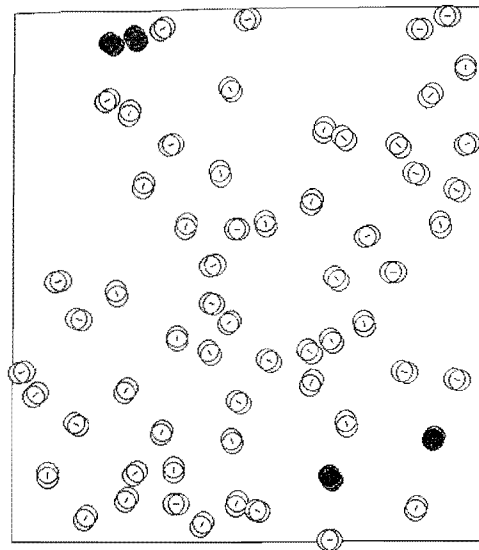


FIG. 6. Snapshot of a 64-dumbbell systems at a density of $n = 0.1\sigma^{-2}$. The central part of a dumbbell is painted gray if its squared particle component for the maximum exponent exceeds 0.06. Similarly, the peripheral part is painted gray if its squared particle component for the minimum exponent exceeds 0.06.

We have shown in Sec. IV that the mean squared projected components allow a rather detailed analysis of the tangent space dynamics for the offset vectors $\delta\Gamma_l$. If one projects into the various subspaces $T\mu_i$ for all dumbbells $i = 1, \dots, N$ as suggested in Sec. III, one obtains squared coefficients $\delta_{\mu_i,l}^2(t)$ which, for brevity, we refer to as the instantaneous “squared particle components.” Summed over all particles they obey $\sum_{i=1}^N \delta_{\mu_i,l}^2(t) = 1$. In Fig. 6 we show a snapshot ($N=64, n=0.1, d=0.25$) where the color of the dumbbells is chosen according to the squared particle component for the tangent vectors of the conjugate exponent pair $l=1$. The central part of a dumbbell i is painted black if the component associated with the *maximum* exponent is larger than 0.06, and a dumbbell is given a gray peripheral part if the same condition holds for the most *negative* exponent. In Fig. 7 a similar snapshot is shown where the color code now refers to the squared particle components of the two tangent vectors associated with the positive and negative conjugate exponents λ_{100} and λ_{285} . From Figs. 6 and 7 it is observed (i) that the respective tangent vectors have significant components only in subspaces belonging to a few particles, (ii) that these particles are localized in space and grouped in clusters, (iii) that the clusters for the two conjugate exponents, both labeled by the same index l , are *identical*. This is a consequence of the symplectic nature of a pairwise collision; and (iv) that the clusters for different conjugate pairs are also different. The observation (i) was already made by us in Ref. 32 for soft-disk systems in nonequilibrium steady states involving up to 102400 particles. It is generally found that the localization of this active cluster for a given l is much more pronounced for larger and denser systems.

The active zone has the appearance of a collective mode, which moves through the fluid, but remains localized. We were unable to relate it to other hydrodynamic fields such as

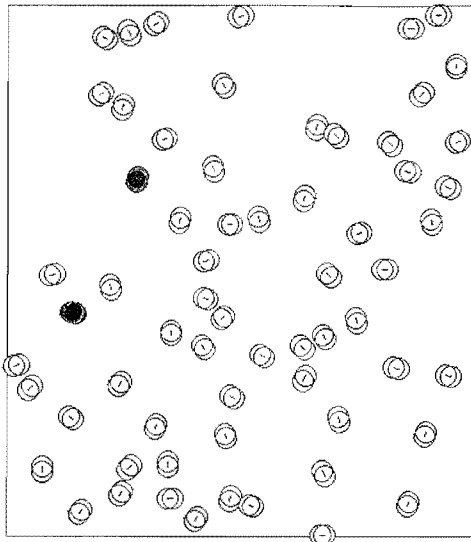


FIG. 7. As in Fig. 6 where the central and peripheral coding refers to the squared particle components associated with the positive exponent λ_{100} and its conjugate negative exponent λ_{285} .

the temperature. This localization is a consequence of two mechanisms: first, the delta-vector components of two colliding molecules after a collision are linear functions of their components before the collision and have a chance to grow significantly only if their size before the collision was already far above average. Second, the renormalization after such a collision tends to reduce the (already small) components of the other noncolliding particles even further. Thus, the competition for the maximum growth of "their" tangent vector components favors the collision pair with the largest components. It is interesting to note that the "clock variables," introduced by van Zon *et al.* for the computation of the maximum exponent,²³ assume the role of the tangent-vector components for the various particles and that, not surprisingly, they single out a few "active" particles arranged in localized clusters similar to the structures found here.

ACKNOWLEDGMENTS

We thank Professor H. van Beijeren, Professor J. R. Dorfman, and Dr. Ch. Dellago for valuable discussions. We

also gratefully acknowledge the support from the Fonds zur Förderung der wissenschaftlichen Forschung under Grant No. P11428-PHY. Work at the Lawrence Livermore National Laboratory was performed under the auspices of the University of California, through Department of Energy Contract No. W-7405-eng-48.

- ¹E. Ott, *Chaos in Dynamical Systems* (Cambridge University Press, Cambridge, 1993).
- ²H. A. Posch and W. G. Hoover, *Phys. Rev. A* **88**, 473 (1988).
- ³H. A. Posch and W. G. Hoover, *Phys. Rev. A* **89**, 2175 (1989).
- ⁴B. L. Holian, W. G. Hoover, and H. A. Posch, *Phys. Rev. Lett.* **59**, 10 (1987).
- ⁵Wm. G. Hoover and H. A. Posch, *Chaos* **8**, 366 (1998).
- ⁶D. J. Evans and G. P. Morriss, *Statistical Mechanics of Nonequilibrium Liquids* (Academic, London, 1990).
- ⁷W. G. Hoover, *Computational Statistical Mechanics* (Elsevier, Amsterdam, 1991).
- ⁸I. Borzsák, András Baranyai, and H. A. Posch, *Physica A* **229**, 94 (1996).
- ⁹H. A. Posch, W. G. Hoover, and B. L. Holian, *Ber. Bunsenges. Phys. Chem.* **94**, 250 (1990).
- ¹⁰Ch. Dellago and H. A. Posch, *Physica A* **230**, 364 (1996).
- ¹¹H.-H. Kwon and B.-Y. Park, *J. Chem. Phys.* **107**, 5171 (1997).
- ¹²V. Mehra and R. Ramaswamy, *Phys. Rev. E* **56**, 2508 (1997).
- ¹³P. Butera and G. Caravati, *Phys. Rev. A* **36**, 962 (1987).
- ¹⁴Ch. Dellago and H. A. Posch, *Physica A* **237**, 95 (1997).
- ¹⁵Ya. G. Sinai, *Int. J. Bifurcation Chaos Appl. Sci. Eng.* **6**, 1137 (1996).
- ¹⁶R. Livi, A. Politi, and S. Ruffo, *J. Stat. Phys.* **19**, 2033 (1986).
- ¹⁷Ch. Dellago, H. A. Posch, and W. G. Hoover, *Phys. Rev. E* **53**, 3694 (1996).
- ¹⁸Ch. Dellago and H. A. Posch, *Physica A* **240**, 68 (1997).
- ¹⁹D. J. Searles, D. J. Evans, and D. J. Isbister, *Physica A* **240**, 96 (1997).
- ²⁰G. Benettin, L. Galgani, A. Giorgilli, and J.-M. Strelcyn, *Meccanica* **15**, 9 (1980).
- ²¹I. Shimada and T. Nagashima, *Prog. Theor. Phys.* **61**, 1605 (1979).
- ²²H. van Beijeren, J. R. Dorfman, H. A. Posch, and Ch. Dellago, *Phys. Rev. E* **56**, 5272 (1997).
- ²³R. van Zon, H. van Beijeren, and Ch. Dellago, *Phys. Rev. Lett.* **80**, 2035 (1998).
- ²⁴I. Borzsák, H. A. Posch, and A. Baranyai, *Phys. Rev. E* **53**, 3694 (1996).
- ²⁵Lj. Milanović, H. A. Posch, and Wm. G. Hoover (unpublished).
- ²⁶M. P. Allen, D. Frenkel, and J. Talbot, *Comput. Phys. Rep.* **9**, 301 (1989).
- ²⁷V. I. Oseledec, *Trans. Moscow Math. Soc.* **19**, 197 (1968).
- ²⁸A. Wolf, J. B. Swift, H. L. Swinney, and J. A. Vastano, *Physica D* **16**, 285 (1985).
- ²⁹B. Fuchssteiner, Automath, MuPAD-Group, University of Paderborn, Germany; electronic mail: benno@uni-paderborn.de.
- ³⁰M. D'Alessandro and A. Tenenbaum, *Phys. Rev. E* **52**, R2141 (1995).
- ³¹W. G. Hoover and H. A. Posch, *Phys. Rev. E* **51**, 273 (1995).
- ³²Wm. G. Hoover, K. Boercker, and H. A. Posch, *Phys. Rev. E* **57**, 3911 (1998).